

Statics and dynamics of selfish interactions in distributed service systems

F. Altarelli,^{1,2} A. Braunstein,^{1,3,2} and L. Dall'Asta^{1,2}

¹*DISAT and Center for Computational Sciences, Politecnico di Torino,
Corso Duca degli Abruzzi 24, 10129 Torino, Italy*

²*Collegio Carlo Alberto, Via Real Collegio 30, 10024 Moncalieri, Italy*

³*Human Genetics Foundation, Via Nizza 52, 10126 Torino, Italy*

We study a class of games which model the competition among agents to access some service provided by distributed *service units* and exhibit congestion and frustration phenomena when service units have limited service capacity. We propose a technique, based on the cavity method of statistical physics, to characterize the full spectrum of Nash equilibria of the game. The analysis reveals a large variety of equilibria, with very different statistical properties. Natural selfish dynamics, such as best-response, usually tend to large-utility equilibria, even though those of smaller utility are exponentially more numerous. Interestingly, the latter can be actually reached by selecting the initial conditions of the best-response dynamics close to the saturation limit of the service unit capacities. We also study a more realistic stochastic variant of the game by means of a simple and effective approximation of the (quenched) average over the random parameters, showing that the properties of the equilibrium space are qualitatively similar to the deterministic case.

I. INTRODUCTION

Health care, education and communications are public sectors in which administrations traditionally face the problem of organizing distributed service systems. Service provision is *distributed* because a possibly large number of post-offices, hospitals, or libraries is maintained over the territory in order to allow all citizens to have potential access to the services. Moving from public economics to information technology and computer networks, one can easily find other examples of distributed service provision. File-storage and file-sharing systems maintain servers (or mirrors) arranged all around the world to offer faster download to clients. Large wireless networks in airports and university campuses count dozens of access points ensuring connection to thousands of potential users.

In all such systems the *users* can access the service through one of a set of distributed *service units*, that is managed by a unique central authority, i.e. the *service provider*. In this respect the problem looks like a standard optimization problem, with the administrator seeking for the optimal resource allocation, in which all users are served and the load on the units is balanced minimizing the costs. On the other hand, the strategic, non-cooperative character of the problem is evident from the fact that users are self-interested agents. Every user wants to be served from the service unit that is most convenient to her, because of a smaller load, geographical proximity or a higher quality of service. As resources are normally limited, the individual utilities of the users depend, directly or indirectly on the usage that others do of the same service unit. Service units have typically different quality of service, and the latter may also depend on the workload of the unit at the time of service. For instance, when waiting lists become too large, choosing the best hospital or the most efficient public office could become inconvenient. In file-sharing systems the time required to download files depends on the number of requests to the same server. When too many users download from the same server, the quality of service deteriorates. Wireless access points serve users according to a round robin, providing one opportunity to transmit at each user during a cyclic time frame of finite duration. This physical constraint imposes a limitation on the number of users that can be connected to a single access point at the same time. Similar phenomena of “congestion” occur in every distributed service provision system and make the organizational problem a game theoretic one, in which the non-cooperative behavior of the users causes degradation with respect to a centralized optimal solution.

The outcome of any strategic interaction among rational agents can be predicted and classified using the concept of *Nash equilibrium*, which describes a situation in which no player has incentive to unilaterally deviate from the chosen strategy profile. As a result of the simultaneous maximization of all individual utilities, a game can admit more than one Nash equilibrium. The existence of multiple Nash equilibria is particularly common in strategic decision problems in disordered and networked systems, where the number of different Nash equilibria can even scale exponentially with the number of players. As many other systems in computer science [1] and network economics [2], distributed service provision systems can admit a large multiplicity of Nash equilibria.

Whenever multiple equilibria exist, all of them are equally rational and there is no a priori way to state which one would be chosen by the agents. This lack of predictive power is usually resolved by introducing some refinement of the concept of Nash equilibrium or some criterium of equilibrium selection. A reasonable assumption is that the selected Nash equilibrium should be the outcome of a dynamical process in which agents may interact several times. However, no dynamical rule is universal and different ones lead to equilibria with possibly very different properties. In order

to quantify how much the efficiency of a system degrades due to the selfish behavior of its agents, computer scientist introduced the concepts of *Price of Anarchy* [3] and *Price of Stability* [4]. The Price of Anarchy is the ratio between the utility of the social optimum and the utility of the worst equilibrium, while the Price of Stability is the ratio between the utility of the social optimum and that of the best equilibrium. In fact, these quantities only give bounds on the equilibrium landscape, providing no further information on its structure. A better knowledge of the equilibrium landscape is crucial to devise reasonable criteria of equilibrium selection and to discriminate between the outcomes of different dynamical rules. Such information can be then exploited to design effective self-enforcing mechanisms, for example by means of incentives, to move the system away from bad equilibria towards the most efficient ones.

It was recently proved possible to investigate the whole landscape of Nash equilibria in multi-agent games, such as public goods games on networks [5–7], by mapping the equilibrium condition on a constraint-satisfaction problem and then analyzing it using efficient message-passing algorithms based on the cavity method from statistical physics [8–10]. Here we adopt this approach to study a simple model of distributed service provision that is strictly related to classes of games that have been studied thoroughly in computer science such as *selfish load balancing* [11] and *congestion games* [12, 13]. A common property of all these games is that they admit a potential function [14]: Nash equilibria are thus the local minima of such a potential and it is possible to show that the optimal assignment is also a Nash equilibrium. As the set of strategies is finite and the potential function increases during the best-response dynamics, the latter always converges to a Nash equilibrium. It is however not clear how much efficient Nash equilibria (i.e. of large aggregate utility) obtained from best-response are compared to those obtained using different dynamical rules and how much the answer depends on the initial conditions. Moreover, the real self-organization processes of the agents are not exactly best-response processes and their details are normally not known, therefore a complete analysis cannot be restricted to a single dynamics. We bring evidence of the richness of the equilibrium landscape by describing the full set of Nash equilibria using a statistical mechanics analysis and comparing it with the typical fixed-points of different dynamics. We also study the effects of correlating the users’ utilities with the loads they bring to the system. Finally we generalize the analysis to a stochastic case, in which the agents are present with a given probability. To do this, we introduce a new algorithmic approximation technique to perform the required quenched average over the stochastic parameters on single instances.

The paper is organized as follows. In Section II, we describe the distributed service provision game, the Nash equilibrium condition and some general properties of the equilibria. The mapping of the Nash equilibrium conditions on a constraint-satisfaction problem is presented in Section III, together with its factor graph representation while the derivation of the Belief Propagation equations used to solve the constraint-satisfaction problem is given in Section IV. A detailed analysis of the equilibrium landscape on random instances in the deterministic case and the comparison with the results of explicit dynamics are presented in Section V. Finally, the analysis is generalized to a stochastic environment (i.e. to instances in which agents can either participate to the game or not, the choice being made at random with some known probability). A simple but effective message passing approximation to compute the quenched average of observables over the stochastic parameters is presented in Section VI, while numerical results are reported in Section VII.

II. THE SERVICE PROVISION GAME

In the service provision game, there are two types of entities: users and service units. Each user benefits from being serviced by one service unit, with each service unit providing her a different utility. A user would prefer being serviced by the unit that provides her the largest utility. However, service units have finite capacity, so in certain cases the first choice for a given user can be unavailable. An instance of the service provision game is represented by a bipartite graph $G = (U, S; E)$ as in Fig. 1, where $U = \{1, \dots, N\}$ is the set of users, $S = \{1, \dots, M\}$ is the set of service units, and an edge (ua) is present in E if and only if the service unit a is accessible to the user u . We associate to each edge $(ua) \in E$ a positive weight w_{ua} , that represents the *load* placed on service unit a by user u , and a positive quantity v_{ua} representing the (utility) *value* that u gives to the service provided by a . We also associate a capacity C_a to each service unit a , representing the maximum load it can serve. In a general setup, values and weights are heterogeneous, as the same user u may provide a different load w_{ua} to different service units a and obtain different levels of satisfaction v_{ua} . In some cases, the two quantities on the same edge (ua) can be positively or negatively correlated.

The *action* of a user u corresponds to the choice among the M possible service units. For each edge (ua) , we introduce a binary variable $x_{ua} \in \{0, 1\}$, such that $x_{ua} = 1$ iff user u is served by service unit a . The action of user u is given by the binary vector $\mathbf{x}_u = (x_{u1}, x_{u2}, \dots, x_{uM})$ in which at most one component can be equal to 1, i.e. it

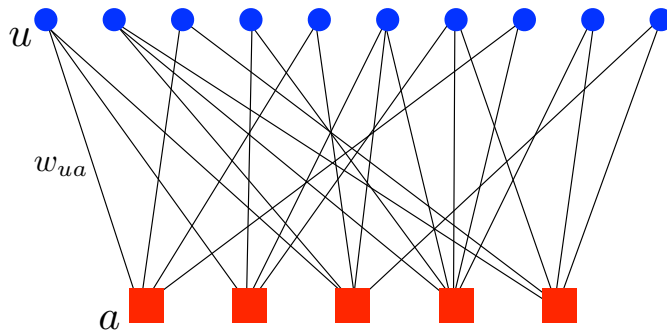


FIG. 1: Bipartite graph representing an instance of the service provision game, with weights w_{ua} between users $u \in \mathbf{U}$ and service units $a \in \mathbf{S}$.

satisfies the condition

$$\sum_{a \in \partial u} x_{ua} \leq 1 \quad (\forall u \in \mathbf{U}), \quad (1a)$$

where $\partial u \subset \mathbf{S}$ denotes the neighbors of u on the graph. The capacity constraints can be written as

$$\sum_{u \in \partial a} x_{ua} w_{ua} \leq C_a \quad (\forall a \in \mathbf{S}). \quad (1b)$$

The utility for user u is simply

$$U_u = \begin{cases} \sum_{a \in \partial u} x_{ua} v_{ua} & \text{if (1) are satisfied,} \\ -\infty & \text{otherwise.} \end{cases} \quad (2)$$

An action profile $\mathbf{x} = \{\mathbf{x}_u\}_{u \in \mathbf{U}}$ is a (pure strategy) *Nash equilibrium* of the service provision game if no user can increase her utility by unilaterally switching to a different service unit, i.e. for each user u

$$U_u(\mathbf{x}) \geq \max_{\mathbf{x}'} U_u(\mathbf{x}', \mathbf{x}_{\setminus u}) \quad (3)$$

where $U_u(\mathbf{x}', \mathbf{x}_{\setminus u}) = U_u(\mathbf{x}_1, \dots, \mathbf{x}_{u-1}, \mathbf{x}', \mathbf{x}_{u+1}, \dots, \mathbf{x}_N)$.

Let us call X^N the action space, a game is an *exact potential game* if there exists a potential function $V : X^N \rightarrow \mathbb{R}$, such that for each user u

$$U_u(\mathbf{x}_u, \mathbf{x}_{\setminus u}) - U_u(\mathbf{x}'_u, \mathbf{x}_{\setminus u}) = V(\mathbf{x}_u, \mathbf{x}_{\setminus u}) - V(\mathbf{x}'_u, \mathbf{x}_{\setminus u}). \quad (4)$$

The service provision game is a potential game that admits the aggregate utility $U = \sum_u U_u$ as an exact potential V . This statement is easy to prove because the benefit that a user receives for being connected to a service unit does not directly depend on the actions of the others but only on the availability of the unit itself. It follows that when a user moves to a different service unit, her action does not affect the utilities of all the other users, even of those that are disconnected from the system. In this respect, a better measure of social welfare should take into account both the aggregate utility U and the number D of disconnected users, e.g. in a linear combination $U - \alpha D$. In practice, the problem can be simplified slightly as follows. We can add a new virtual service unit for each user with unlimited capacity and negative value $-\alpha$. Because of the negative contribution to the utility, this new “*unservice unit*” will be chosen only as a last resort, when all real units are saturated and the user would be otherwise disconnected. In this modified game, users are always connected (but connection to the *unservice unit* represents disconnection in the original game) and their total utility satisfies $U' = U - \alpha D$. In any case, if a user can improve her utility with a feasible move, this will not affect the social welfare enjoyed by other users, and the total social welfare will necessarily improve, which means that a configuration which is not a Nash equilibrium cannot be the social optimum. The Nash equilibria of the service provision game are in one-to-one relation with the local maxima of the potential V , i.e. of the aggregate utility U . This can be verified by defining the *best response* relations. For a user u , the best response to the actions of the other users consists in choosing the action that maximizes her own utility given the choice of the others, that is \mathbf{x}_u is the best response for u to the remaining action profile $\mathbf{x}_{\setminus u}$ if

$$\mathbf{x}_u = \arg \max_{\mathbf{x}'} U_u(\mathbf{x}', \mathbf{x}_{\setminus u}). \quad (5)$$

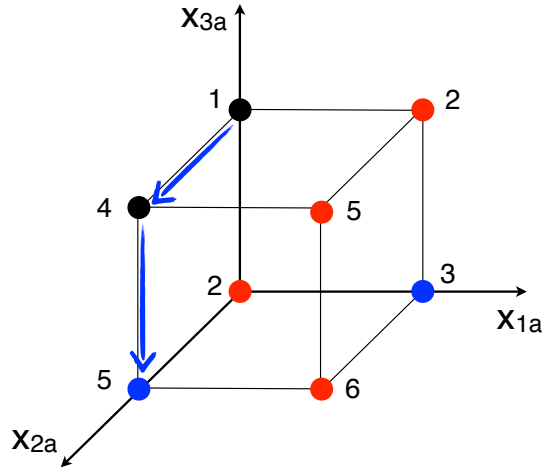


FIG. 2: Binary representation (x_{1a}, x_{2a}, x_{3a}) of the action space for the example presented in Section II with 3 users and 2 service units. Each vertex corresponds to a possible configuration: non-feasible configurations, that violate capacity constraints, are marked in red, Nash equilibria are marked in blue. The value of the aggregate utility is also reported for each configuration. The blue arrows indicate an improvement path obtained by best response from $(0, 0, 1)$ to the Nash equilibrium $(0, 1, 0)$.

In a potential game with discrete actions and finite strategy space, the potential does not decrease during the iteration of best-response reactions, and the latter always converge to a pure Nash equilibrium in a finite number of steps [14]. Because of this property, the path in the action space generated by the iteration of the best response relations is often called the *improvement path*.

Let us review all these properties in a simple example of service provision game composed of three users $U = \{1, 2, 3\}$ and two service units $S = \{a, b\}$. The weights are $w_{1a} = 3, w_{1b} = 1, w_{2a} = 1, w_{2b} = 2$, and $w_{3a} = 1, w_{3b} = 2$, while the values given to the service are $v_{1a} = 2, v_{1b} = 1, v_{2a} = 3, v_{2b} = 0$, and $v_{3a} = 0, v_{3b} = 1$. Service units have capacities $C_a = 3, C_b = 4$. In this example, the values of weights and capacities are defined in such a way that users can always be connected to one of the two service units. In this case, for each user u either x_{ua} or x_{ub} will be equal to 1 and the action profile simplifies considerably. Since $x_{ub} = 1 - x_{ua}$, the aggregate utility can be written as

$$U = \sum_{u=1}^3 \sum_a (v_{ua}x_{ua} + v_{ua}(1 - x_{ua})) = 2 + x_{1a} + 3x_{2a} - x_{3a}, \quad (6)$$

and the capacity constraints on the loads of the service units are

$$\ell_a = \sum_u w_{ua}x_{ua} = 3x_{1a} + x_{2a} + x_{3a} \leq 3 \quad (7a)$$

$$\ell_b = \sum_u w_{ub}x_{ub} = 5 - x_{1a} - x_{2a} - x_{3a} \leq 4. \quad (7b)$$

In the reduced action space (x_{1a}, x_{2a}, x_{3a}) , the feasible action profiles are $(1, 0, 0)$, $(0, 1, 0)$, $(0, 0, 1)$, $(0, 1, 1)$, and the Nash equilibria are $(0, 1, 0)$ and $(1, 0, 0)$ (see Fig.2). Suppose the system is in the feasible configuration $(0, 0, 1)$, with aggregate utility $U = 1$ and let the users perform best response. User 1 will not move from unit b to unit a , although the latter could provide a better service, because of the capacity constraint on a ; user 3 will not move from a to b for the same reason. For user 2, it is instead convenient to leave service unit b and connect to a , because $v_{2a} = 3 > v_{2b} = 0$ and the weight $w_{2b} = 1$ will not cause any capacity violation on a . The new configuration $(0, 1, 1)$ has aggregate utility $U = 4$ but it is not a Nash equilibrium. Indeed, user 3 can now increase her own utility by switching from unit a to unit b , which has now sufficient spare capacity. The action profile $(0, 1, 0)$ is a fixed-point for the best response dynamics and a pure Nash equilibrium of the game. Notice that the Nash equilibrium is also a local maximum for the aggregate utility ($U = 5$). There is another Nash equilibrium in which user 1 is connected to unit a , while both 2 and 3 use unit b . This Nash equilibrium has a low aggregate utility $U = 2$ but it saturates the capacities of both units (loads $\ell_a = 3$ and $\ell_b = 4$). Interestingly, the best Nash equilibrium induces loads $\ell_a = 1$ on unit a and $\ell_b = 3$ on unit b , that are instead far below the capacity limits. We will see that this phenomenology is a general feature of equilibria in the service provision game.

When there are many users and service units, with different weights, service values and capacities, the number of Nash equilibria grows exponentially with the size of the instance and they will show a wide spectrum of properties. In Section III and Section IV, we will put forward a method, based on statistical mechanics techniques, to study the properties of all Nash equilibria, classifying them depending on different quantities. In many realistic situations, however, the instance of the game theoretic problem changes over time, because the agents could follow very complex temporal activity patterns. An example is given by wireless service provision: a provider can have information of all users potentially connected to the network, but it will not be able to anticipate the exact time at which they will be connected and the duration of the connections. One can imagine that agents could leave the system and come back, using different service units depending on their preference and the current availability. In the absence of any precise information on the dynamics of the agents, one could be tempted to use a standard approach in games with *incomplete information*: the lack of information about the complexity of agents' activity is summarized into a set of stochastic parameters $\{t_u\}_{u \in \mathbf{U}}$. If $t_u = 0$ the user u is *inactive* (meaning that u doesn't participate to the game), whereas $t_u = 1$ if she is *active* (meaning that u participates to the game). The probability that user u is active ($t_u = 1$) is p_u , which we assume to be known, and it is independent on the state of other users. However, under the standard assumptions of incomplete information, agents do not know the exact realization of the stochastic parameters, but only their probability distribution. Agents maximize an expected utility and the notion of Nash equilibrium is replaced by that of Bayesian Nash equilibrium [2]. In the present setup, the major drawback of the formulation with incomplete information is that it does not describe correctly the behavior of the users. In realistic situations, users connect to the system and possibly rearrange their decisions on the base of the current instance of the problem, until they reach an equilibrium. In other words, we expect that users play a game of complete information on the deterministic instance corresponding to a single realization of the stochastic parameters $\{t_u\}_{u \in \mathbf{U}}$. The knowledge of the probabilities p_u is instead relevant in order to sample over many realizations of the stochastic parameters and evaluate the average properties of the Nash equilibria of the game. In Section VI, we will show that our methods can be generalized in order to average the properties of the Nash equilibria over the realization of the stochastic parameters without resorting to sampling techniques.

III. REPRESENTATION AS A CONSTRAINT-SATISFACTION PROBLEM

A. Deterministic case

The topology of the graph together with the values of the parameters $\{w_{ua}, (ua) \in \mathbf{E}\}$, $\{v_{ua}, (ua) \in \mathbf{E}\}$ and $\{C_a, a \in \mathbf{S}\}$ completely define an instance of the game. In the following, we shall assume that all the weights, utilities and capacities are positive integers. In the following we will show that the Nash equilibrium conditions can be mapped on the solutions of a constraint-satisfaction problem. In order to do that, we introduce a convenient set of variables $y_{ua} \in \{\mathbf{U}, \mathbf{A}, \mathbf{S}\}$ associated to the edges $(ua) \in \mathbf{E}$ of the graph, representing both the choice of user u and the availability of service unit a as follows:

$$y_{ua} = \begin{cases} \mathbf{U} & \text{if } a \text{ is unavailable to } u, \\ \mathbf{A} & \text{if } a \text{ is available to } u, \text{ but } u \text{ is not served by } a, \\ \mathbf{S} & \text{if } u \text{ is served by } a. \end{cases} \quad (8)$$

In order for a configuration of the constraint satisfaction problem to be a valid configuration in the service provision game, it must satisfy the following constraints. First, each user can be served by at most one service unit

$$\sum_{a \in \partial u} \mathbb{1}[y_{ua} = \mathbf{S}] \leq 1 \quad (\forall u \in \mathbf{U}) \quad (9a)$$

where $\mathbb{1}[\textit{proposition}]$ is the indicator function for *proposition*, which is equal to 1 if *proposition* is true and 0 otherwise. Second, the total load on each service unit cannot exceed its capacity:

$$\sum_{u \in \partial a} w_{ua} \mathbb{1}[y_{ua} = \mathbf{S}] \leq C_a \quad (\forall a \in \mathbf{S}). \quad (9b)$$

Third, a service unit a is available to a user u (not currently served by a) if and only if a has a spare capacity sufficient to serve u :

$$\{y_{ua} = \mathbf{A}\} \Leftrightarrow \left\{ w_{ua} + \sum_{v \in \partial a \setminus u} w_{va} \mathbb{1}[y_{av} = \mathbf{S}] \leq C_a \right\} \wedge \{y_{ua} \neq \mathbf{S}\} \quad (\forall (ua) \in \mathbf{E}). \quad (9c)$$

A valid configuration is a Nash equilibrium if it satisfies the further condition that each user is served by the best available service unit, or equivalently that if a service unit a is available to user u but not used by u , then u must be served by some other service unit b with a utility at least as large as a 's:

$$\{y_{ua} = \mathbf{A}\} \Leftrightarrow \left\{ \exists b \in \partial u : \{y_{ub} = \mathbf{S}\} \wedge \{v_{ub} \geq v_{ua}\} \right\} \wedge \{y_{ua} \neq \mathbf{U}\} \quad (\forall (ub) \in \mathbf{E}). \quad (9d)$$

The sets of conditions (9) are the hard constraints characterizing the solutions of the constraint-satisfaction problem under study, that are the Nash equilibria of the service provision game. Although all Nash equilibria are a priori equally rational, we expect that they could have different properties, therefore we shall be interested to compute the average value \bar{O} of some extensive observable $O(y)$ with a uniform measure over the Nash equilibria:

$$\bar{O} = \frac{1}{\mathcal{N}} \sum_y O(y) \mathcal{C}(y) \quad (10)$$

where \mathcal{N} is the total number of Nash equilibria and $\mathcal{C}(y)$ is equal to 1 if the conditions (9) are satisfied and 0 otherwise, so that $\mathcal{N} = \sum_y \mathcal{C}(y)$. Some interesting observables will be the aggregate utility

$$U(y) = \sum_{(ua) \in \mathbf{E}} v_{ua} \mathbb{1}[y_{ua} = \mathbf{S}], \quad (11)$$

the total number of users who are disconnected (i.e. who are not served by any service unit)

$$D(y) = \sum_{u \in \mathbf{U}} \mathbb{1} \left[\sum_{a \in \partial u} \mathbb{1}[y_{ua} = \mathbf{S}] = 0 \right], \quad (12)$$

or the aggregate unutilized (spare) capacity

$$C^*(y) = \sum_{a \in \mathbf{S}} \left\{ C_a - \sum_{u \in \partial a} w_{ua} \mathbb{1}[y_{ua} = \mathbf{S}] \right\} = \sum_{a \in \mathbf{S}} C_a - L(y) \quad (13)$$

where $L(y)$ is the aggregate load.

In the following we shall also be interested in characterizing the Nash equilibria which correspond to a given value of some observable $O(y)$. In order to do this we shall follow a canonical approach, introducing a Gibbs measure

$$P(y|\mu) = \frac{1}{Z(\mu)} \exp\{\mu O(y)\} \mathcal{C}(y) \quad (14)$$

where the chemical potential μ allows to select the average value of the observable O over the distribution $P(y|\mu)$, and where the partition function $Z(\mu) = \sum_y \exp\{\mu O(y)\} \mathcal{C}(y)$ is a normalization. Notice that for $\mu = 0$ we recover the uniform distribution over all Nash equilibria. The entropy

$$S(\mu) = - \sum_y P(y|\mu) \log P(y|\mu) \quad (15)$$

provides a measure of the number of Nash equilibria corresponding to the average value $O(\mu)$ of $O(y)$, defined as

$$O(\mu) = \sum_y O(y) P(y|\mu). \quad (16)$$

In the following, all quantities averaged over the distribution $P(y|\mu)$ will be denoted using a calligraphic fonts, such as $\mathcal{U}, \mathcal{D}, \mathcal{C}^*$.

B. Stochastic case

An instance of the stochastic service provision game is completely determined by the topology of the graph and the values of the parameters $\{w_{ua}, (ua) \in \mathbf{E}\}$, $\{v_{ua}, (ua) \in \mathbf{E}\}$, $\{C_a, a \in \mathbf{S}\}$ and $\{p_u, u \in \mathbf{U}\}$. A configuration of the stochastic game is described by the pair (t, y) where $t = \{t_u, u \in \mathbf{U}\}$ represents the activity of users, and

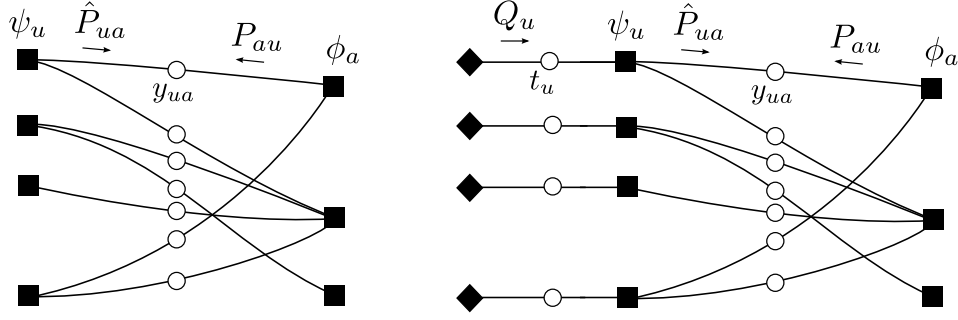


FIG. 3: Factor graph representation. Left: For the deterministic case the set of constraints is $\mathcal{C}(y) = \prod_{u \in \mathbf{U}} \psi_u(y_u) \prod_{a \in \mathbf{S}} \phi_a(y_a)$. Right: For the stochastic case, the factor graph includes mirror nodes (black lozanges) and the corresponding messages $Q_u(t_u)$. The set of constraints is $\mathcal{C}(y, t) = \prod_{u \in \mathbf{U}} \psi_u(y_u, t_u) \prod_{a \in \mathbf{S}} \phi_a(y_a)$.

$y = \{y_{ua}, (ua) \in \mathbf{E}\}$ represents their actions. The conditions (9) for y to be a Nash equilibrium remain unchanged, except for the first one, which becomes

$$\sum_{a \in \partial u} \mathbb{1}[y_{ua} = \mathbf{S}] \leq t_u \quad (\forall u \in \mathbf{U}). \quad (17)$$

When considering the average properties of an instance of stochastic service provision game, for instance the average value $\langle O \rangle$ of an observable $O(y)$, we must perform a double average: over all the Nash equilibria corresponding to a given realization of the parameters $t = \{t_u, u \in \mathbf{U}\}$, and over the realization of t :

$$\langle O \rangle = \sum_t P(t) \frac{1}{\mathcal{N}(t)} \sum_y O(y) \mathcal{C}(y, t) \quad (18)$$

where $\mathcal{N}(t)$ is the number of Nash equilibria corresponding to a given realization of t , and where $\mathcal{C}(y, t)$ is 1 if y is a Nash equilibrium for t and 0 otherwise.

IV. BELIEF PROPAGATION EQUATIONS FOR THE DETERMINISTIC CASE

We denote $y_u = \{y_{ua}, a \in \partial u\}$ the set of variables y_{ua} on the edges incident on $u \in \mathbf{U}$, and similarly for $y_a = \{y_{ua}, u \in \partial a\}$. We consider a factor graph with the same topology as the bipartite graph $\mathbf{G} = (\mathbf{U}, \mathbf{S}; \mathbf{E})$ representing the instance, with factor nodes $\psi_u(y_u)$ associated to the users $u \in \mathbf{U}$ and enforcing the constraints (9a) and (9d), and factor nodes $\phi_a(y_a)$ associated to the service units $a \in \mathbf{S}$ and enforcing the constraints (9b) and (9c) (Figure 3, left-hand panel).

We introduce the BP messages $P_{au}(y_{ua})$ traveling on the edge $(ua) \in \mathbf{E}$ from the service unit a to the user u , and $\hat{P}_{ua}(y_{ua})$ traveling in the opposite direction. Notice that since all the variables have connectivity 2 there is no difference between variable-to-factor and factor-to-variable messages. In the following we derive the BP equations for the uniform distribution over all Nash equilibria, i.e. setting $\mu = 0$ in (14). It is straightforward to introduce a bias related to the value of any extensive observable $O(x)$ as in (14). Formally, the BP equations can be written as

$$P_{au}(y_{ua}) = \frac{1}{z_a} \sum_{\{y_{va}, v \in \partial a \setminus u\}} \phi_a(y_a) \prod_{v \in \partial a \setminus u} \hat{P}_{va}(y_{va}), \quad (19a)$$

$$\hat{P}_{ua}(y_{ua}) = \frac{1}{z_u} \sum_{\{y_{ub}, b \in \partial u \setminus a\}} \psi_u(y_u) \prod_{b \in \partial u \setminus a} P_{bu}(y_{ub}) \quad (19b)$$

where z_u and z_a are normalization constants, which we shall omit in the following writing the updates up to a multiplicative constant. The number of terms in the sums grows exponentially with the connectivity of the nodes, and we need to derive some update equations which can be computed efficiently.

Let us begin with the update equation for the users nodes. The constraint (9a) requires that either 0 or 1 of the y 's can be equal to \mathbf{S} , all the other y 's being equal to \mathbf{U} or \mathbf{A} . Moreover, the constraint (9d) requires that the y 's associated to edges with a higher utility values than the edge with y equal to \mathbf{S} have y equal to \mathbf{U} . We shall consider

separately the three cases $y_{ua} = \mathbf{U}$, \mathbf{A} and \mathbf{S} . When $y_{ua} = \mathbf{U}$, it is possible that all the y 's are \mathbf{U} . Otherwise, exactly one of them must be equal to \mathbf{S} , and we must sum over the possible choices for this y . The remaining y 's must be \mathbf{U} if they correspond to a larger value than the one with $y = \mathbf{S}$ and otherwise they can be either \mathbf{U} or \mathbf{A} . We obtain

$$\widehat{P}_{ua}(\mathbf{U}) \propto \prod_{b \in \partial u \setminus a} P_{bu}(\mathbf{U}) + \sum_{b \in \partial u \setminus a} P_{bu}(\mathbf{S}) \prod_{\substack{c \in \partial u \setminus a: \\ v_{uc} > v_{ub}}} P_{bu}(\mathbf{U}) \prod_{\substack{d \in \partial u \setminus \{a,b\}: \\ v_{ud} \leq v_{ub}}} [P_{du}(\mathbf{U}) + P_{du}(\mathbf{A})]. \quad (20a)$$

When $y_{ua} = \mathbf{A}$, one of the other y 's must be equal to \mathbf{S} , and it must have a value at least as large as v_{ua} , and we obtain

$$\widehat{P}_{ua}(\mathbf{A}) \propto \sum_{\substack{b \in \partial u \setminus a: \\ v_{ub} \geq v_{ua}}} P_{bu}(\mathbf{S}) \prod_{\substack{c \in \partial u \setminus a: \\ v_{uc} > v_{ub}}} P_{bu}(\mathbf{U}) \prod_{\substack{d \in \partial u \setminus \{a,b\}: \\ v_{ud} \leq v_{ub}}} [P_{du}(\mathbf{U}) + P_{du}(\mathbf{A})]. \quad (20b)$$

Finally, when $y_{ua} = \mathbf{S}$, all the other y 's must be either \mathbf{U} or \mathbf{A} , and they can be \mathbf{A} only if their value is not larger than v_{ua} , giving

$$\widehat{P}_{ua}(\mathbf{S}) \propto \prod_{\substack{b \in \partial u \setminus a: \\ v_{ub} > v_{ua}}} P_{bu}(\mathbf{U}) \prod_{\substack{c \in \partial u \setminus \{a,b\}: \\ v_{uc} \leq v_{ua}}} [P_{cu}(\mathbf{U}) + P_{cu}(\mathbf{A})]. \quad (20c)$$

All these products can be computed efficiently, providing an efficient update.

In order to compute the update for service unit nodes, we introduce, for any subset $\mathbf{K} \in \partial a$ of the edges incident on service unit a , the convolution

$$\mathcal{P}_{\mathbf{K}}(S, T) = \sum_{\{y_{ua}, u \in \mathbf{K}\}} \mathbb{1} \left[\sum_{u \in \mathbf{K}} w_{ua} \mathbb{1}[y_{ua} = \mathbf{S}] = T \right] \prod_{u \in \mathbf{K}} \mathbb{1} \left[\{y_{ua} = \mathbf{U}\} \Leftrightarrow \{w_{ua} + S > C_a\} \wedge \{y_{ua} \neq \mathbf{S}\} \right] \widehat{P}_{ua}(y_{ua}) \quad (21)$$

which can be computed efficiently thanks to the relation

$$\mathcal{P}_{\mathbf{K} \cup \mathbf{L}}(S, T) = \sum_{T_1, T_2} \mathbb{1}[T_1 + T_2 = T] \mathcal{P}_{\mathbf{K}}(S, T_1) \mathcal{P}_{\mathbf{L}}(S, T_2) \quad (22)$$

valid for any disjoint subsets \mathbf{K} and \mathbf{L} of the incident edges, starting from the single edge quantities

$$\mathcal{P}_u(S, T) = \begin{cases} \widehat{P}_{ua}(\mathbf{S}) & \text{if } T = w_{ua} \text{ (for any } S) \\ \widehat{P}_{ua}(\mathbf{A}) & \text{if } T = 0 \text{ and } S \leq C_a - w_{ua} \\ \widehat{P}_{ua}(\mathbf{U}) & \text{if } T = 0 \text{ and } S > C_a - w_{ua} \\ 0 & \text{otherwise} \end{cases} \quad (u \in \partial a). \quad (23)$$

In terms of $\mathcal{P}_{\partial a \setminus u}(S, T)$ we have:

$$P_{au}(\mathbf{U}) \propto \sum_S \mathbb{1}[C_a - w_{ua} < S \leq C_a] \mathcal{P}_{\partial a \setminus u}(S, S) \quad (24a)$$

$$P_{au}(\mathbf{A}) \propto \sum_S \mathbb{1}[0 \leq S \leq C_a - w_{ua}] \mathcal{P}_{\partial a \setminus u}(S, S) \quad (24b)$$

$$P_{au}(\mathbf{S}) \propto \sum_S \mathbb{1}[0 \leq S \leq C_a - w_{ua}] \mathcal{P}_{\partial a \setminus u}(S + w_{ua}, S) \quad (24c)$$

from which it is clear that we need to compute $\mathcal{P}_{\partial a \setminus u}(S, T)$ for any $T \in \{0, 1, \dots, C_a\}$ and $S \in \{0, 1, \dots, C_a\}$.

V. NUMERICAL RESULTS ON A RANDOM ENSEMBLE OF DETERMINISTIC INSTANCES

A. Definition of the ensemble of instances

We consider a random ensemble of deterministic instances with N users and M service units, all with capacity C . For any user u and any service unit a , the edge (ua) is present with probability q , and the parameters w_{ua} and v_{ua}

are integers extracted from the maximum entropy distribution over the range $\{w_{\min}, \dots, w_{\max}\} \times \{v_{\min}, \dots, v_{\max}\}$ conditioned on a given value of Pearson's correlation coefficient

$$c = \frac{\langle w_{ua}v_{ua} \rangle - \langle w_{ua} \rangle \langle v_{ua} \rangle}{\sqrt{\langle w_{ua}^2 \rangle - \langle w_{ua} \rangle^2} \sqrt{\langle v_{ua}^2 \rangle - \langle v_{ua} \rangle^2}} \quad (25)$$

(the reason for this choice will be clear shortly). Such an ensemble is fully specified by the parameters N , M , C , q , w_{\min} , w_{\max} , v_{\min} , v_{\max} and c . These parameters will determine the qualitative features of the phenomenology as follows.

The total available capacity $\hat{C} = MC$ can be compared to a lower and an upper bound for the total capacity required to service all users, defined as

$$\hat{C}^- = \sum_u \min_{a \in \partial u} w_{ua}, \quad \hat{C}^+ = \sum_u \max_{a \in \partial u} w_{ua}. \quad (26)$$

When the total available capacity \hat{C} is large compared to \hat{C}^+ the system is under-constrained and the solution is trivial: every user can be served by the service unit with the highest utility, and every service unit has some spare capacity, so that suboptimal configurations in which some users are not fully satisfied are not Nash equilibria. At the opposite end of the spectrum, when \hat{C} is small compared to \hat{C}^- , many users receive no service at all, and the users who are served typically enjoy a low utility. As \hat{C} goes to zero the number of equilibria decreases, and it reaches 1 when \hat{C} is smaller than the smallest weight and all the users are unserved, which is again a trivial regime. The interesting regime corresponds to intermediate values $\hat{C}^- \lesssim \hat{C} \lesssim \hat{C}^+$, when some of the capacity constraints are saturated and some other are not.

For any value of the total capacity \hat{C} , the level of tightness of the constraints depends on two more parameters. The first is the average connectivity of users, determined by q : for larger values of q , users will have more alternative service units to chose from, and the system will be less constrained. The second is the minimum value of the weights w_{\min} : spare capacity on individual service units smaller than w_{\min} cannot be used, so that for larger values of w_{\min} typical configurations will be more inefficient and the system will be more constrained.

Finally, the correlation c between weight and utility is a measure of the degree of competition among users: when c is close to -1 , users prefer to be served by those service units over which they place a low burden, minimizing the capacity they subtract to other users, and the competition is mild; when c is close to 0, users' preferences are independent of the load they place on service units, and on the impact this has on the capacity available to other users; finally, when c is close to $+1$, weights and utility values tend to coincide (up to an affinity transformation), and users try to subtract as much capacity as possible to other users, so that the competition is harsh.

B. Average values of the observables: \mathcal{U} , \mathcal{D} and C^*

We study the average values of the relevant observables (i.e. the total utility, the total number of disconnected users, and the total spare capacity) as a function of the capacity C of individual service units and of the correlation c between the weight w_{ua} and the values v_{ua} on each edge $(ua) \in \mathbf{E}$, keeping fixed the remaining parameters. The range of values for C corresponds to a total capacity \hat{C} between 8000 and 12000, spanning the relevant range of values defined by the bounds (26) with expected values $\hat{C}^- = 6581$ and $\hat{C}^+ = 14418$. Results of numerical simulations are shown in Figure 4.

For small values of C , the total utility \mathcal{U} decreases with c as expected. However, for larger values there is a surprising inversion of this dependency: larger values of c , which give rise to harsher competition between users, correspond to *higher* values of the average total utility. In particular, when the individual capacity is $C = 60$, the average total utility for $c = -1$ is 4306 ± 12 , while for $c = +1$ it is 6190 ± 9 , with a 43.8% increase. It is also surprising that, for values of c close to -1 , the average total utility *does not* increase monotonically with the capacity C : on the contrary, for $c = -1$ it reaches a maximum value 4896 ± 35 for $C = 47$ (not plotted in Figure 4), well above the value corresponding to $C = 60$, which is 4306 ± 12 .

The average total number of disconnected users \mathcal{D} shows, as expected, a strong dependency on the capacity C , but surprisingly it is almost independent on the correlation c . Since the social welfare depends on both \mathcal{U} and \mathcal{D} , we obtain the striking result that, provided the capacity C is large enough, a harsher competition between users, in which each user prefers to subtract to other users as many of the available resources as possible, gives rise on average to a higher social welfare than a milder form of competition, in which users prefer to minimize the amount of resources they subtract to other users.

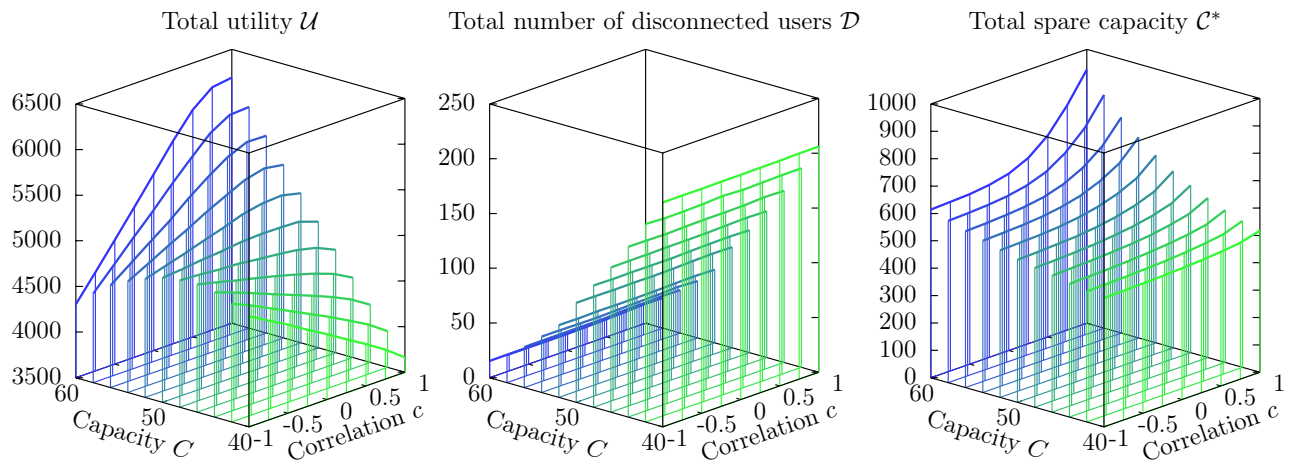


FIG. 4: Average values \mathcal{U} , \mathcal{D} and \mathcal{C}^* of the observables as a function of the capacity C_a of service units and the correlation c between weight and utility on individual edges. The other parameters are $N = 1000$, $M = 200$, $q = 0.04$, $w_{\min} = 6$, $w_{\max} = 15$, $v_{\min} = 1$ and $v_{\max} = 10$. Each data point, corresponding to a vertical line, is an average over ~ 115 instances, and the standard deviations are of the order of the width of the lines.

Finally, the average total spare capacity \mathcal{C}^* increases monotonically with C , which could be easily expected, and also with c : as the average weight placed on service units by individual users increases, it becomes more difficult to use the capacity efficiently, and a larger fraction of capacity is wasted (even though a sizable number of users are disconnected!).

C. Comparison with explicit dynamics

We compare the average values of the observables obtained by averaging uniformly over all Nash equilibria with Belief Propagation with the results of the explicit simulation of three interesting dynamics which converge to Nash equilibria:

- *Greedy (G)* – The first dynamics consists in extracting a random permutation of the users and assigning to each one in turn the service unit with the highest utility among the available ones. Obviously, at the end of the assignment we have a Nash equilibrium, in which some users (who came early in the permutation) enjoy a very high utility while some other users (who came late) are either disconnected or with very low utility.
- *Best response (BR)* – The second dynamics starts from a random initial condition, extracted by forming again a random permutation of the users and assigning to each one in turn a service unit extracted uniformly at random among the available ones. The dynamics then proceeds in rounds. In each round, a random permutation of the users is extracted, and each user in turn attempts to improve their utility (possibly freeing some capacity at the service unit previously serving them, and allowing other users to use it). The dynamics stops when no user can improve their utility (and therefore the configuration is a Nash equilibrium).
- *Best response from “bad” initial condition (BRB)* – The third dynamics is identical to the second one, except for the choice of the initial condition: instead of selecting uniformly at random their service unit among the available ones, each user initially selects the *worst* one among the available ones (i.e. the one with the lowest utility), in turn and according to a random permutation of the users. Then, they follow the best response dynamics.

Numerical results for the average values of the observables \mathcal{U} , \mathcal{D} and \mathcal{C}^* as a function of the correlation c (for fixed values of the remaining parameters) are shown in Figure 5 for BP and for the three dynamics.

The most striking feature of these plots is that the uniform average over Nash equilibria computed by BP is very far from the averages computed by sampling over the three dynamics, even in the region where the three dynamics give very similar results (i.e. for $-0.5 \leq c \leq 0.5$). It appears very clearly that the three dynamics we considered are strongly biased towards “good” equilibria. In particular, when $-0.5 \leq c \leq 0.25$ all the dynamics converge to equilibria which are nearly optimal, with values of \mathcal{U} very close to the expected value of the theoretical upper bound $U^+ = \sum_u \max_{a \in \partial u} v_{ua} = 9843$, while BP finds values which grow almost linearly with c (again, indicating that

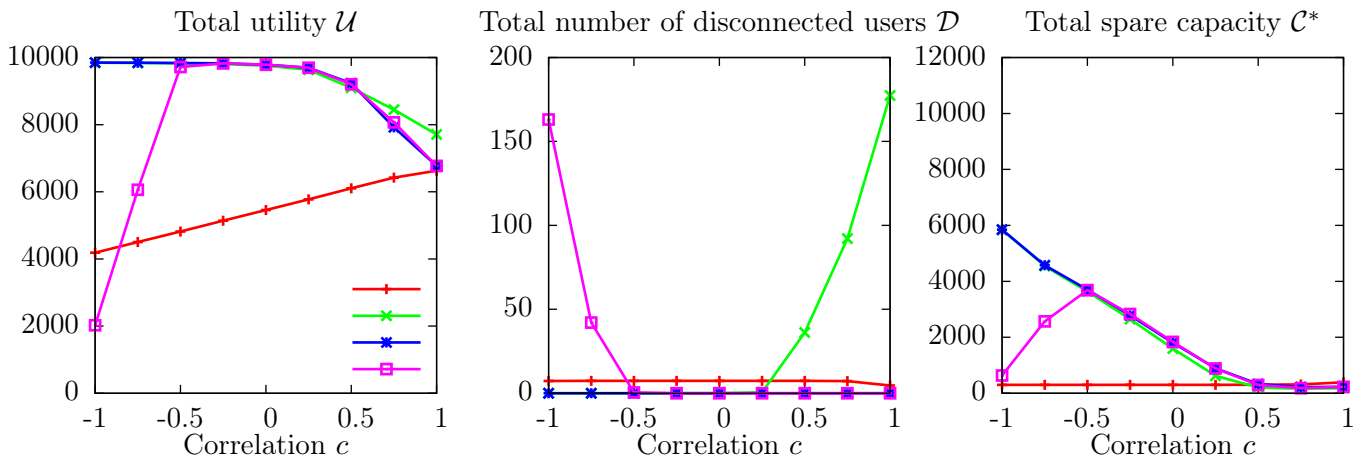


FIG. 5: Average values \mathcal{U} , \mathcal{D} and \mathcal{C}^* of the observables as a function of the correlation c between weight and utility on individual edges. The other parameters are $N = 1000$, $M = 100$, $C = 120$, $q = 0.2$, $w_{\min} = 6$, $w_{\max} = 15$, $v_{\min} = 1$ and $v_{\max} = 10$. Each data point is an average over ~ 40 instances, and for each instance, each dynamics is realized 10 000 times. The average value of each observable is computed over the instances and over the realizations. The standard deviations (of the averages over the realizations of the dynamics across different instances) are much smaller than symbol sizes.

harsher competition leads on average to higher total utility) in the range from 4817 ± 22 (where the error is the standard deviation of the average of the observable across different instances) obtained for $c = -0.5$ to 5775 ± 19 obtained for $c = 0.25$, which is between 41.3% and 51.8% less than the optimum.

When $c = -1$, BRB actually finds equilibria with much lower average total utility than BP: in the initial condition of BRB users are connected to service units with low utility values, which for $c = -1$ correspond to high weights, so that service units are saturated (as confirmed by the low value of the average total spare capacity $\mathcal{C}^* = 635 \pm 70$), and the configuration is close to an equilibrium, which the best response part of the dynamics reaches without improving much the value of \mathcal{U} . The average total utility of BRB increases very sharply as c passes from -1 to -0.5 , where it is already very close to the optimum, indicating that when the anticorrelation between weights and values is imperfect, the initial configuration is no longer close to an equilibrium (as confirmed by the much larger values of \mathcal{C}^*), and during the best response part of the dynamics the configuration can “escape” and reach a good equilibrium. As c increases further, all the dynamics find near optimal equilibria up to $c = 0.25$ and then the value of \mathcal{U} starts to decrease significantly (as one would normally expect). When $c = 1$ BP finds results that are similar to the two best response dynamics, but still far from greedy. In the full range of c the average total utility found by BP increases almost linearly with c .

The results found by different dynamics for the average total number of disconnected users \mathcal{D} is even more heterogeneous. With BR, all users are *always* connected provided $c < 0.75$, and for larger values of c the value of \mathcal{D} is never larger than 6.2×10^{-3} . This is in sharp contrast with the results of BRB, which finds a relatively high number of disconnected users when c is small (with $\mathcal{D} = 163 \pm 3$ for $c = -1$), and with the results of greedy, which finds a relatively large number of disconnected users when c is large (with $\mathcal{D} = 177 \pm 2$ for $c = 1$). By contrast, BP finds a value of $\mathcal{D} = 7.4 \pm 0.2$ which is constant for $-1 \leq c \leq 0.5$, and then decreases to $\mathcal{D} = 4.6 \pm 0.2$ for $c = 1$. In the region $-0.5 \leq c \leq 0.25$ the three dynamics find negligible values of \mathcal{D} , again indicating a strong bias towards high utilities in the equilibria they reach.

Finally, the average value of the total spare capacity \mathcal{C}^* found by BP is almost constant and very low across the range of values of c , with $\mathcal{C}^* = 302 \pm 1$ for $c \leq 0.5$ and increasing slightly for larger values of c to 393 ± 2 for $c = 1$. It appears very clearly that the uniform average over Nash equilibria is dominated by configurations with utilities that are much smaller than the optimal one, but which are “locked” by a lack of spare capacity. The same thing seems to happen to BRB for $c \leq -0.75$, and to other dynamics (but to a much lesser extent) for $c \geq 0.5$.

D. Analysis of the entropy vs. utility curve for individual instances

In order to clarify the (sometimes counterintuitive) phenomena discussed in the previous paragraphs, we analyzed in detail individual instances with different values of the correlation $c \in \{-1, -0.5, 0, 0.5, 1\}$ (with the other parameters taking the same values as in the previous paragraph). Specifically, we computed with BP the thermodynamic entropy $S(\mu)$ and the average total utility $\mathcal{U}(\mu)$ for a large number of values of the chemical potential μ , both positive and

c	BP	MS	BP	MS	U^+	PoA
-1	800.00	800	9 867.97	9 868	9 868	12.34
-0.5	856.89	857	9 839.98	9 840	9 840	11.48
0	1 064.44	1 057	9 837.02	9 858	9 858	9.33
0.5	1 763.94	1 782	9 851.02	9 853	9 855	5.53
1	6 169.17	6 139	7 962.71	7 965	9 874	1.30

TABLE I: Comparison of the minimum and maximum utilities found by Belief Propagation as $\mu \rightarrow \pm\infty$ with the values found by Max-Sum, which allows to explicitly find an equilibrium configuration of extreme utility, and with the upper bound U^+ defined in the main text. The last column shows the price of anarchy computed from the MS values.

negative. This allows to plot $S(\mu)$ vs. $\mathcal{U}(\mu)$, providing a measure of the number of Nash equilibria corresponding to a given value of the total utility. We compared this to a sampling of the equilibria obtained with the three dynamics previously introduced: greedy (G), best response from random initial condition (BR) and best response from “bad” initial conditions (BRB). The results are shown in Figure 6.

For $c = -1$ a first order transition is present: the free energy $\mu F(\mu) = \mu\mathcal{U}(\mu) + S(\mu)$ has a discontinuous derivative at $\mu^* = 0.3453$, and the entropy vs. utility curve consists of two branches separated by a wide gap. The thermodynamically stable branch is the low-utility one for $\mu < \mu^*$ and the high-utility one for $\mu > \mu^*$. In the high utility branch, both $\mathcal{U}(\mu)$ and $S(\mu)$ converge to a constant limit as $\mu \rightarrow +\infty$, varying very little between $\mu = 1$ (with $\mathcal{U} = 9\,867.23$ and $S = 681.33$) and $\mu = 10/3$ (with $\mathcal{U} = 9\,867.97$ and $S = 680.20$). The limit value for \mathcal{U} coincides with the upperbound for the utility $U^+ = \sum_u \max_{a \in \partial u} v_{ua} = 9\,868$, and the limit value of S gives the logarithm of the number of Nash equilibria with $\mathcal{U} = U^+$, indicating that this upperbound is feasible and that the number of optimal equilibria is exponentially large. In fact, the three dynamics G, BR and BRB are all capable of finding equilibria with $\mathcal{U} = U^+$. We also found optimal equilibria with $\mathcal{U} = U^+$ with Max-Sum, the zero temperature (or infinite μ , in this case) version of BP (see Table I for the full results of Max-Sum). For $\mu > 10/3$, BP converges to a fixed point with unphysical properties ($\mathcal{U} > U^+$ and $S < 0$). The high utility branch continues for $\mu < \mu^*$, and it is possible to explore it with BP starting with $\mu > \mu^{\text{BP}} = 0.7812$ and decreasing it in small steps, allowing BP to converge between each step (and keeping the messages when μ changes). Notice that for $\mu^* < \mu < \mu^{\text{BP}}$ the stable branch is the high utility one, but BP converges to (unstable) solutions in the low utility branch. The values of \mathcal{U} and S tend to a constant limit as $\mu \rightarrow 0^+$, with $\mathcal{U} = 9\,863.67$ and $S = 682.82$ for $\mu = 0.1$ which become $\mathcal{U} = 9\,862.67$ and $S = 682.87$ for $\mu = 10^{-6}$. The results obtained with greedy show that Nash equilibria can be found with utilities as small as 9 857, which is smaller than the limit value found by BP.

The low utility branch has much larger values of the entropy, and therefore it dominates the statistics. When $\mu = 0$ the distribution is unbiased (i.e. uniform over all Nash equilibria) and $\mathcal{U} = 4\,182.40$ is the average utility over all Nash equilibria while $S = 2\,598.23$ is the logarithm of the total number of equilibria. When $\mu^* < \mu$ the low utility branch is unstable, but it can be studied with BP as explained above, starting with a small value of μ and increasing it gradually up to $\mu = \mu^{\text{BP}}$, where the solution found by BP jumps discontinuously to the high utility branch. For negative values of μ , the distribution is biased towards Nash equilibria with lower-than-average utilities. As $\mu \rightarrow -\infty$ both \mathcal{U} and S tend to a constant limit, with $\mathcal{U} = 800.16$ and $S = 580.09$ at $\mu = -10$ which become $\mathcal{U} = 800.00$ and $S = 578.34$ at $\mu = -200/3$, after which BP starts to converge to an unphysical fixed point with zero utility and negative entropy. The average spare capacity for $\mu \leq -10$ is exactly zero, indicating that an exponential number of configurations exist with $\mathcal{U} = 800$ and which use all the available capacity. In fact, when $c = -1$ the edges with the lowest utility, $v_{\min} = 1$, also have the highest weight, $w_{\max} = 15$, so that if 800 users are using edges with $v = 1$ and $w = 15$ the total utility will be 800 and the total capacity used will be 12 000, with no spare capacity. Such a configuration can be easily found with Max-Sum, and we have verified that it exists. Equilibria with very low utilities can also be found by dynamics: in 93.2% of 10^6 runs BRB converges to equilibria with utilities between 1 135 and 1 734. In the remaining cases it manages to “escape” from the low utility branch and to reach optimal or nearly optimal equilibria.

The most striking feature of the S vs. \mathcal{U} curve for $c = -1$ is the presence of a very wide gap, covering the range $\mathcal{U} \in [4\,463.88, 9\,862.78]$. This gap can be intuitively explained with the following argument. When $c = -1$, two type of equilibria exist: in “good” equilibria, users are served by service units with high utility, and therefore low weight, which ensures that the capacity is sufficient for (almost) all users; in “bad” equilibria, users are served by service units with low utility, and therefore high weight, so that there is no spare capacity to permit a dynamical transition to a good equilibrium. The maximum spare capacity in bad equilibria is approximately $M(w_{\min} - 1)$, which in our case is 500, because if the spare capacity were larger than that, at least one of the service units would have enough spare

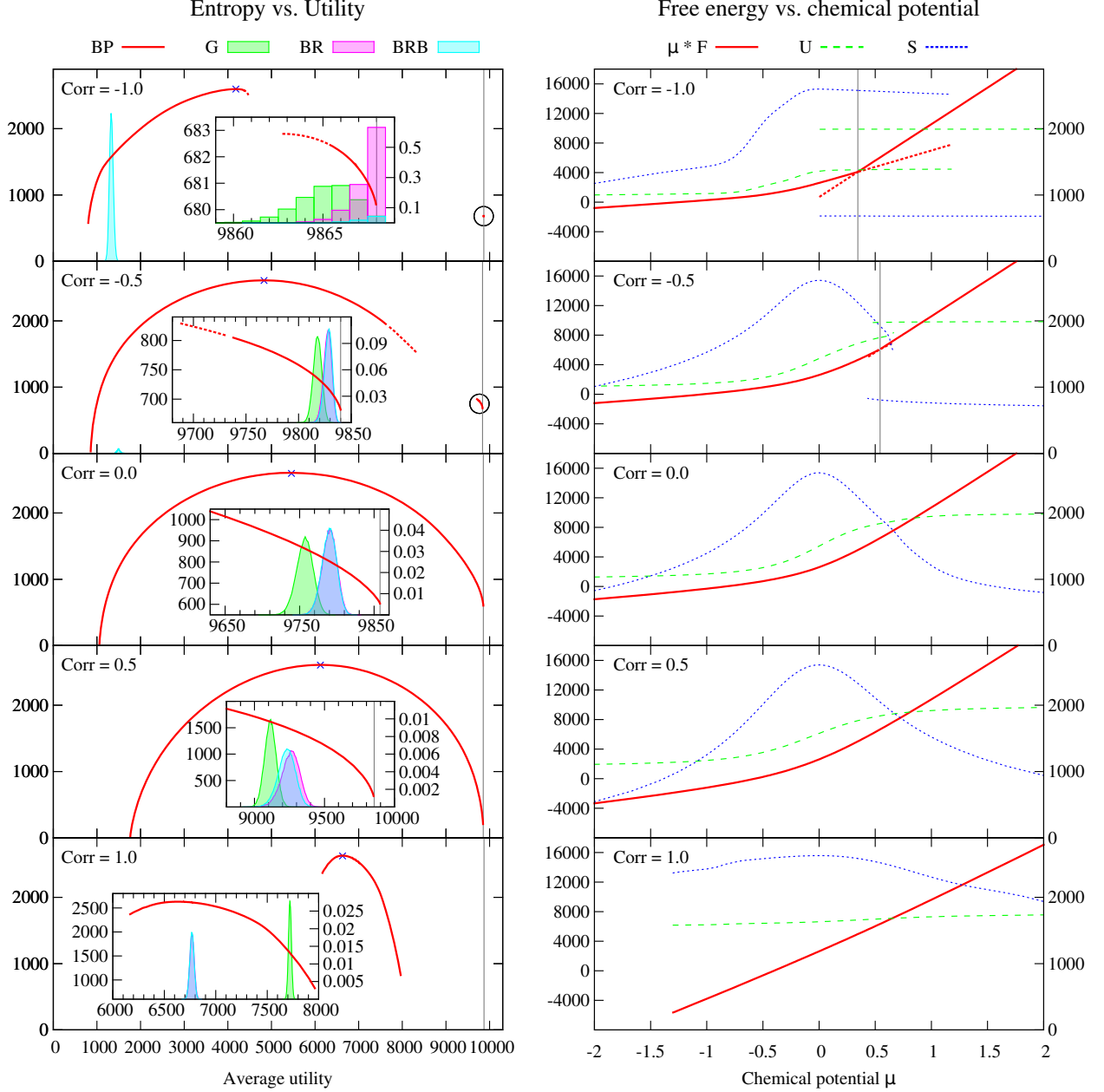


FIG. 6: Computation of the average utility \mathcal{U} and of the entropy S as a function of the chemical potential μ for single instances with correlation c equal to -1 , -0.5 , 0 , 0.5 and 1 (from top to bottom). The other parameters are $N = 1000$, $M = 100$, $C = 120$, $q = 0.2$, $w_{\min} = 6$, $w_{\max} = 15$, $v_{\min} = 1$ and $v_{\max} = 10$. The values of \mathcal{U} and S vs. μ are shown on the right-hand column of plots, together with the Bethe free energy $\mu F = \mu \mathcal{U} + S$. The values of \mathcal{U} and μF are read on the left-hand scale, the values of S on the right-hand one. For $c \leq -0.5$ a first order transition, corresponding to a discontinuity in the first derivative of the free energy, is clearly visible. The critical value μ^* is marked by a vertical grey line, and the thermodynamically unstable branches of the free energy are dotted. The entropy is plotted as a function of the average utility on the left-hand column of plots. For $c \leq -0.5$ the entropy curve has two branches, separated by a wide gap (the high utility branches, which cover a small interval of utilities, are shown in detail in the insets, and they are highlighted by a black circle in the main plots). Dotted lines correspond to the thermodynamically unstable branches of the free energy. For $c \geq 0$ the entropy curve is uninterrupted. The blue crosses at the top of each curve represent the values obtained with $\mu = 0$, i.e. the uniform average over all Nash equilibria, and they always coincide with the maximum of the entropy. The histograms represent the distribution of the total utilities found by the dynamics G, BR and BRB. The number of runs for each dynamics is always 10^5 , except for BRB with $c = -1$ where it is 10^6 . The frequency of each value of utility can be read on the right-hand scale of the insets. The gray vertical lines are upper bounds to the total utility defined as $U^+ = \sum_u \max_{a \in \partial u} v_{ua}$.

capacity to serve a user with the minimum weight, i.e. with the maximum utility, and this user would switch to it. (The spare capacity can be larger than 500 only if there are some service units connected only to edges with weight larger than w_{\min} , which is very unlikely in our case given that the average connectivity of service units is 200, and that the probability that an edge has minimum weight is 0.1). If all the users are served, the total load L , that is the sum of the used weights, is related to the total utility U by the simple relation $U + L = N(v_{\min} + w_{\max}) = 16\,000$, so the maximum utility corresponds to the minimum weight (i.e. 11 500, given that the spare capacity cannot be larger than 500) which gives 4 500. If instead there are D users who are disconnected (i.e. who are not being served), the relation between U and L becomes $U + L = (N - D)(v_{\min} + w_{\max})$, and the utility can only decrease. So, in bad equilibria utilities must be smaller than 4 500. On the other hand, in optimal equilibria, nearly all users have the maximum utility $v_{\max} = 10$, which corresponds to the minimum weight $w_{\min} = 6$, so the total weight is approximately 6 000, which is half the available capacity. In order for an equilibrium to be good but not optimal, some service unit s must be saturated, so that its spare capacity is smaller than w_{\min} , and some of the users who would prefer to be served by s are forced to accept a lower utility with some other service unit. Even in the extreme case in which half the service units are saturated and the other half are empty, it is very likely that a frustrated user will be able to be served by a service unit with $v_{\max} - 1$, so the maximum utility loss (relative to the optimum) is of the order of 1 000. This gives a lower bound for the utility in good equilibria which is approximately 9 000. Therefore, in the range of utilities between (approximately) 4 500 and 9 000, we expect to find no equilibria.

For $c = -0.5$ the phenomenology and its interpretation are very similar to the case $c = -1$ discussed above. However, the size of the gap in utilities is much reduced (it now covers the range [7 621.00, 9 687.20]), the fraction of runs of BRB which find equilibria with low utilities is much smaller (2.0%), and the entropy corresponding to the minimum utility is now zero, indicating that the number of minima is subexponential. For large utilities the entropy curve ends at $\mathcal{U} = U^+ = 9\,840$ with a large value ($S = 682.16$), and both BR and BRB succeed in finding optimal equilibria. For $c = 0$ and $c = 0.5$ the gap in utilities disappears, and all of the three dynamics we tested always find equilibria with large utilities, but they never achieve the upper bound U^+ , which coincides with the end of the entropy curve (with finite values of S). Finally, for $c = 1$ there is one more significant change in the phenomenology: the entropy curve now covers a much smaller range of utilities, from 6 169.17 to 7 962.71. In particular, optimal equilibria (in which every user enjoys the maximum utility) seem no longer achievable. All the three dynamics find equilibria with utilities in a narrow range, which is very different for G compared to the two best response dynamics (BR and BRB), but which fall in the range of utilities found by BP. We can estimate the range of utilities of equilibria with a simple mean-field argument. For $c = 1$, and with $w_{\max} - w_{\min} = v_{\max} - v_{\min}$, the relation between utility and weight on any edge is $w = v + \delta$, where $\delta = w_{\max} - v_{\max}$. If we denote by \bar{v} the average value of the service utilities and by D the number of disconnected users, the total utility and weight will be given by $U = (N - D)\bar{v}$ and $W = (N - D)(\bar{v} + \delta)$. The maximum utility is obtained by maximizing U with respect to \bar{v} and D subject to the capacity constraint $L \leq MC$, which gives $U = 8\,000$ with $D = 0$ and $\bar{v} = 8$. The minimum utility is obtained by minimizing U subject to the constraint that the average spare capacity does not exceed the average weight (because otherwise the ‘‘average user’’ could improve their utility by switching a service unit with excessive spare capacity), i.e. that $C - L/M \leq \bar{v} + \delta$, which gives $U = 65\,000/11 \simeq 5\,909$ with $D = 0$ and $\bar{v} = 65/11$. The extrema of the range of values found by BP are very close to these bounds.

In summary, this analysis of individual instances allows us to understand in detail the phenomenology we observed, and to draw some general conclusions. First, we find that each one of the three dynamics we tested samples equilibria within a very narrow range of utilities (or possibly two very narrow ranges of utilities, for BRB at $c \leq -0.5$), while the full range of possible equilibria is extremely wide. Second, we clarify the reason for the increase of the average total utility when c increases (i.e. when the competition becomes harsher): in the most numerous equilibria most service units are saturated, which requires the total load L to be close to the capacity, i.e. the maximum possible value for L . As the correlation between weight and utility increases, it becomes more and more difficult to find equilibria with very low utilities, and the average utility increases. And third, our characterization also allows us to estimate the price of anarchy (i.e. the ratio between the utilities of the social optimum, which in the service provision game is always a Nash equilibrium itself, and of the worst possible equilibrium), which decreases smoothly from 12.34 for $c = -1$ to 1.30 for $c = 1$ (see I).

E. Finding Nash equilibria with general values of utility.

The results presented in the last two sections have shown that the best-response dynamics tend to converge towards Nash equilibria with large aggregate utility even when the initial condition is a configuration with the worst possible values of utility (see BRB results in Fig.5), unless the dynamical process gets stuck because of capacity constraints. This is possibly due to the fact that the aggregate utility is a potential function for the game that always increases during the best response dynamics. If the available capacity is large, the rearrangement path due to best response

(usually called “improvement path” in potential games [14]) is long and reaches Nash equilibria with very high utility. In a low capacity regime, instead, the improvement paths is much shorter and the best response dynamics converge after very little utility gain. If so, it should be possible to get stuck at any value of the aggregate utility in the interval of existence indicated by the BP analysis.

This idea was tested by introducing a modified best response dynamics in which the initial conditions could span the whole spectrum of utilities, generalizing the BR and BRB dynamics studied in the Section V C. The initialization process works as follows: in random order, each user u selects an available service unit a with probability $p_{ua} \propto u_{ua}^\gamma$, with $\gamma \in (-\infty, +\infty)$. When all users have attempted to connect to the service system, the configuration is used as the initial condition for the best response dynamics. The standard BR algorithm is obtained for $\gamma = 0$, while the BRB one corresponds to the limit $\gamma \rightarrow -\infty$. For $\gamma \in (-\infty, +\infty)$, we can generate configurations with intermediate utility values between the worst and the best ones. Fig.7 shows some properties of the equilibria found performing best response from such configurations on instances with the same parameters as in the previous section and no correlation between weights and utilities ($c = 0$). For large capacities ($C = 120$ in Fig.7a), the best-response dynamics finds Nash equilibria with very high utility (black circles) independently of the utility of the configuration found during the initialization process (black full line). When decreasing the capacity, the best response dynamics start getting trapped in local maxima (Nash equilibria) close to the initial conditions. Fig.7b shows the case $C = 100$, in which a coexistence of “bad” and “good” equilibria is visible for negative values of γ , that extends up to γ smaller than 4. The fraction of times the system finds “bad” Nash equilibria during the dynamical process increases for lower values of γ (blue dashed curve in Fig.7b). This phenomenon becomes dominant when the capacity is further decreased, as shown in Fig.7c for $C = 80$, in which all realizations of the dynamics get stuck in the lower-utility Nash equilibria. The insets display the average aggregate load on the service units after the initialization process (red full line) and in the Nash equilibria (red squares). It is remarkable that, even though $c = 0$, the more efficient equilibria produce also a slightly lower aggregate load compared to “bad” equilibria.

We have shown that, at least in the low capacity regime, Nash equilibria with any value of the total utility can be obtained using a simple generalization of the best-response dynamics. In a more general case, “bad” equilibria still exist, but the system is not sufficiently constrained and best response manages to find the way to the efficient ones. Interestingly, we checked that instead a BP-guided decimation process (this is a process in which iteratively the action of users are fixed following their computed marginals, conditioned to past choices) can be used to find Nash equilibria at almost any value of the utility where they exist, even for large capacity values.

VI. BELIEF PROPAGATION EQUATIONS FOR THE STOCHASTIC CASE

A. The “mirror message” approximation

In the stochastic case, the average value of the observables (18) is computed as a double average: first over the distribution of Nash equilibria for fixed stochastic parameters t , and then over the realization of t . In physical terms, the average over t is a quenched average. The distribution $P(y, t)$ corresponding to the quenched average is

$$P(y, t) = P(y|t)P(t) = \frac{\mathcal{C}(y, t)}{\mathcal{N}(t)}P(t) \quad (27)$$

where $\mathcal{C}(y, t)$ is the indicator function of the constraints (9), $\mathcal{N}(t) = \sum_y \mathcal{C}(y, t)$ is the number of Nash equilibria as a function of t , and $P(t) = \prod_u P_u(t_u)$ is the distribution of the stochastic parameters t . The annealed approximation of this quenched distribution is given by

$$P^{\text{ann}}(y, t) = \frac{1}{Z^{\text{ann}}} \mathcal{C}(y, t)P(t) \quad (28)$$

where Z^{ann} is a partition function independent of t . $P^{\text{ann}}(y, t)$ can be viewed as an approximation to $P(y, t)$, and it is typically a rather poor one. Perhaps the most striking evidence of their difference is that the marginal for t of $P(y, t)$ is by construction the disorder distribution $P(t)$, while the marginal for t of $P^{\text{ann}}(y, t)$ will be in general different. However, the approximation can be improved drastically in a simple and systematic way (and eventually made exact) with a method already employed by Morita [15, 16], that can be reinterpreted in a natural way in terms of the cavity equations we are employing. Formally, the quenched distribution can be rewritten as

$$P(y, t) = \mathcal{C}(y, t)P(t)e^{\phi(t)} \quad (29)$$

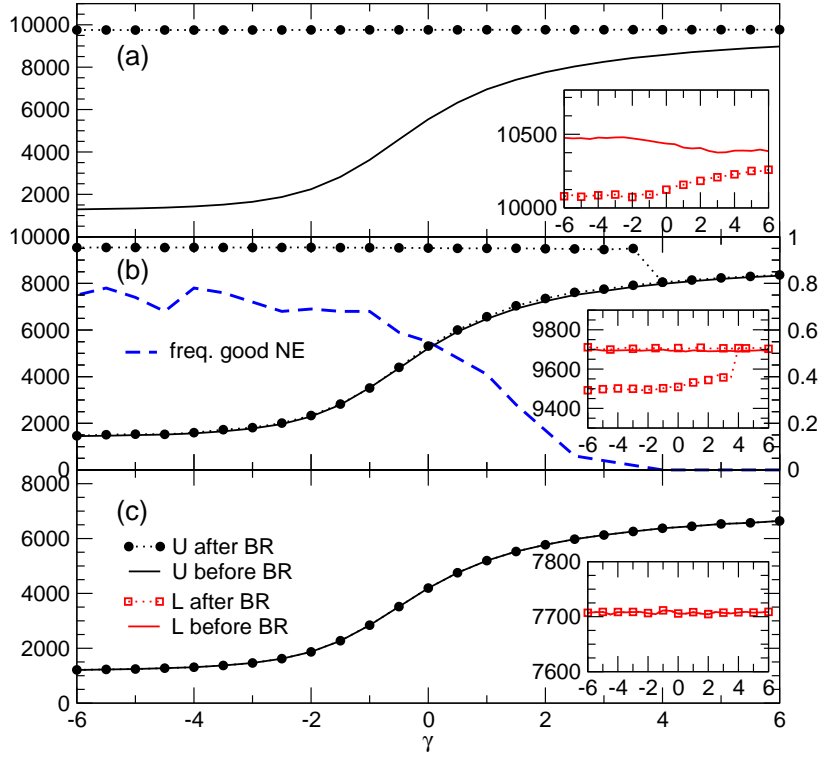


FIG. 7: Average aggregate utility of the initial configuration (black full line) and of the Nash equilibria found by best response (black circles) as a function of the parameter γ and for different values of the capacity $C = 120$ (panel A), 100 (B), 80 (C). The initial load of the units (red dashed line) and the load in the Nash equilibria (red squares) is also reported. The inset displays a magnified plot of the loads, showing that efficient Nash equilibria also induce a decrease in the load on the service units. In panel B we also report (on a different scale) the frequency of times we found good Nash equilibria in our numerical simulations.

with $\phi(t) = -\log \mathcal{N}(t)$. Since the t 's are N binary variables, the function $\phi(t)$ can be parametrized uniquely as

$$\phi(t) = \lambda + \sum_u \nu_u t_u + \sum_{u < v} \rho_{uv} t_u t_v + \sum_{u < v < w} \omega_{uvw} t_u t_v t_w + \dots \quad (30)$$

where the sum is over the 2^N possible subsets of users. By truncating the sum (30), keeping only the constant term λ , we obtain the annealed approximation (28), where $\lambda = -\log Z_{ann}$ is the free energy of the system. We will employ instead the next order approximation, that corresponds to keeping up to the linear terms:

$$P^{\text{lin}}(y, t) = \frac{1}{Z^{\text{lin}}} \prod_{u \in \mathcal{U}} \mathcal{E}_u(y_u, t_u) P_u(t_u) e^{\nu_u t_u} \prod_{a \in \mathcal{S}} \mathcal{E}_a(y_a). \quad (31)$$

In physical terms, ν_u is a local magnetic field acting on t_u ; but its value is not known *a priori*. Note that (31) has the same factorization we had in the deterministic case, and which can be represented by the factor graph of Figure 3 (right-hand panel), that has the same topology as the graph $\mathbf{G} = (\mathcal{U}, \mathcal{S}; \mathbf{E})$ representing the instance. In order to determine coefficients ν_u , we will impose the constraints the average value of t_u is the same as in the exact expression (27), i.e. the distribution of our disorder variables $P(t_u)$. The marginal of t_u is proportional to $Q_u(t_u) \widehat{Q}_u(t_u)$, where the message $\widehat{Q}_u(t_u)$ is determined by the constraint $\mathcal{E}_u(y_u, t_u)$ and by the messages entering the factor node representing it, and we obtain

$$Q_u(0) = \frac{P_u(0)/\widehat{Q}_u(0)}{P_u(0)/\widehat{Q}_u(0) + P_u(1)/\widehat{Q}_u(1)}, \quad Q_u(1) = \frac{P_u(1)/\widehat{Q}_u(1)}{P_u(0)/\widehat{Q}_u(0) + P_u(1)/\widehat{Q}_u(1)}. \quad (32)$$

These equations have a simple intuitive interpretation: the effect of the message $Q_u \propto P_u/\widehat{Q}_u$ is to counterbalance the bias on t_u induced by \widehat{Q}_u , i.e. by the rest of the system, to restore the correct marginal P_u . We therefore refer to the factor node which determines Q_u as a *mirror* node, and to Q_u as a *mirror message*.

Higher order terms in (30) could in principle be retained. For instance, for the next order, one can expect that the correlation between t_u and t_v will be strongest if u and v are close in the graph. One could use a generalized Belief Propagation scheme [17, 18] to perform the computation by defining appropriate regions on the factor graph (at the cost of a larger computational effort), and imposing that pairwise correlations are identical to the ones of the distribution of the quenched disorder (in our case, connected correlations are zero). In the following we shall only consider the linear approximation (31) because, as we shall verify ex-post, the results it gives are sufficiently accurate.

B. BP equations

The BP equation (24) for $P_{au}(y_{ua})$ remains unchanged, while the BP equation (20) remains the same only if $t_u = 1$. If $t_u = 0$ the constraint on the local configuration of y_u is that y_{ua} can be either 0 or 1 for all $a \in \partial u$. We therefore obtain:

$$\begin{aligned} \widehat{P}_{ua}(\mathbf{U}) \propto Q_u(0) \prod_{b \in \partial u \setminus a} [P_{bu}(\mathbf{U}) + P_{bu}(\mathbf{A})] + \\ + Q_u(1) \left\{ \prod_{b \in \partial u \setminus a} P_{bu}(\mathbf{U}) + \sum_{b \in \partial u \setminus a} P_{bu}(\mathbf{S}) \prod_{\substack{c \in \partial u \setminus a: \\ v_{uc} > v_{ub}}} P_{bu}(\mathbf{U}) \prod_{\substack{d \in \partial u \setminus \{a,b\}: \\ v_{ud} \leq v_{ub}}} [P_{du}(\mathbf{U}) + P_{du}(\mathbf{A})] \right\}, \end{aligned} \quad (33a)$$

$$\begin{aligned} \widehat{P}_{ua}(\mathbf{A}) \propto Q_u(0) \prod_{b \in \partial u \setminus a} [P_{bu}(\mathbf{U}) + P_{bu}(\mathbf{A})] + \\ + Q_u(1) \sum_{\substack{b \in \partial u \setminus a: \\ v_{ub} \geq v_{ua}}} P_{bu}(\mathbf{S}) \prod_{\substack{c \in \partial u \setminus a: \\ v_{uc} > v_{ub}}} P_{bu}(\mathbf{U}) \prod_{\substack{d \in \partial u \setminus \{a,b\}: \\ v_{ud} \leq v_{ub}}} [P_{du}(\mathbf{U}) + P_{du}(\mathbf{A})], \end{aligned} \quad (33b)$$

$$\widehat{P}_{ua}(\mathbf{S}) \propto Q_u(1) \prod_{\substack{b \in \partial u \setminus a: \\ v_{ub} > v_{ua}}} P_{bu}(\mathbf{U}) \prod_{\substack{c \in \partial u \setminus \{a,b\}: \\ v_{uc} \leq v_{ua}}} [P_{cu}(\mathbf{U}) + P_{cu}(\mathbf{A})]. \quad (33c)$$

These updates can be computed as efficiently as their deterministic counterparts (20). One more message exits the factor node u : the message to the variable t_u , which we denote by $\widehat{Q}_u(t_u)$. The corresponding update equation is easily seen to be

$$\widehat{Q}_u(0) \propto \prod_{a \in \partial u} [P_{au}(\mathbf{U}) + P_{au}(\mathbf{A})], \quad (34)$$

$$\widehat{Q}_u(1) \propto \prod_{a \in \partial u} P_{au}(\mathbf{U}) + \sum_{a \in \partial u} P_{au}(\mathbf{S}) \prod_{\substack{b \in \partial u: \\ v_{ub} > v_{ua}}} P_{au}(\mathbf{U}) \prod_{\substack{c \in \partial u \setminus a: \\ v_{uc} \leq v_{ua}}} [P_{cu}(\mathbf{U}) + P_{cu}(\mathbf{A})]. \quad (35)$$

Finally, the update equation for the fields $Q_u(t)$ are obtained by requiring that the marginal for t_u is equal to $P_u(t_u) = p_u t_u + (1 - p_u)(1 - t_u)$:

$$Q_u(0)\widehat{Q}_u(0) \propto 1 - p_u \qquad Q_u(1)\widehat{Q}_u(1) \propto p_u \quad (36)$$

from which we obtain

$$Q_u(0) \propto \frac{(1 - p_u)\widehat{Q}_u(1)}{p_u\widehat{Q}_u(0) + (1 - p_u)\widehat{Q}_u(1)}, \quad (37a)$$

$$Q_u(1) \propto \frac{p_u\widehat{Q}_u(0)}{p_u\widehat{Q}_u(0) + (1 - p_u)\widehat{Q}_u(1)}. \quad (37b)$$

VII. NUMERICAL RESULTS ON RANDOM ENSEMBLES OF STOCHASTIC INSTANCES

A. Definition of the ensemble of instances

The random ensemble of instances is defined as in the deterministic case, with the addition of the probabilities $\{p_u, u \in \mathbf{U}\}$ with which user u is active (i.e. participates to the game), which are extracted uniformly at random in

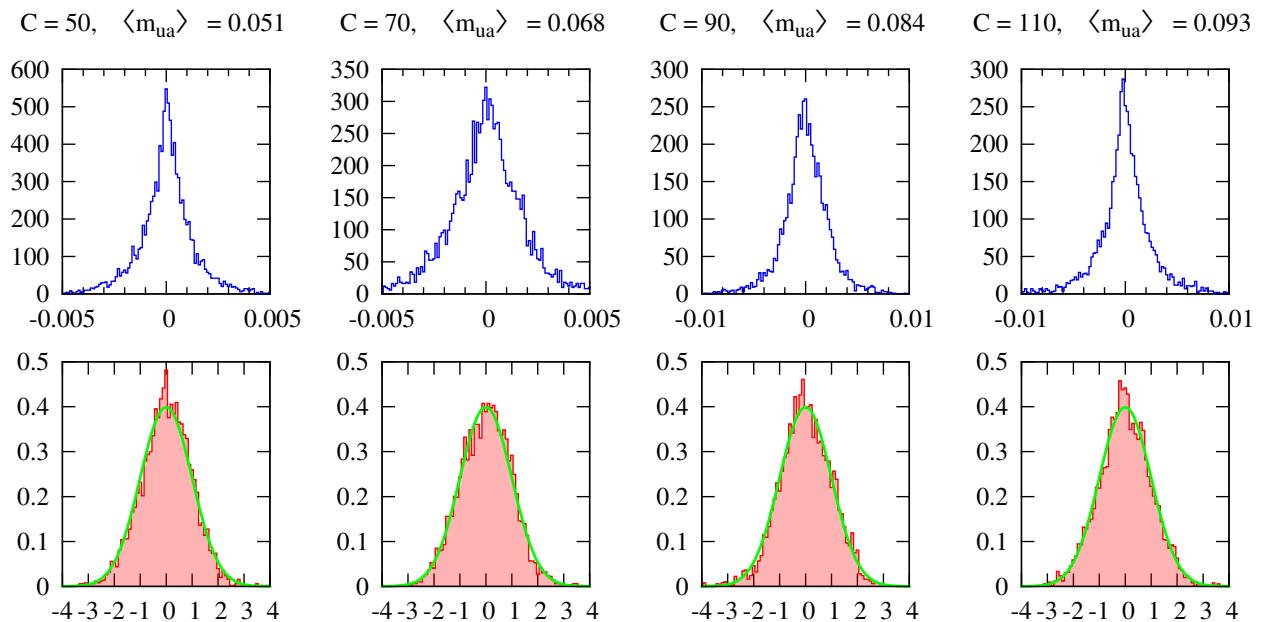


FIG. 8: Distribution of the absolute difference Δ_{ua} between the mirror and sampling estimates of the marginals (top) and of their normalized error $\delta_{ua} = \Delta_{ua}/\sigma_{ua}$ (bottom) for four individual instances with different capacities $C_a = C \in \{50, 70, 90, 110\}$. The other parameters of the instances are $N = 1000$, $M = 50$, $q = 0.1$, $w_{\min} = 6$, $w_{\max} = 15$, $v_{\min} = 1$ and $v_{\max} = 10$ and $c = 0$, and each p_u is extracted uniformly and independently in $]0, 1[$ (these are the values of the parameters we shall consider also in the following Sections). The typical values of the absolute difference are $\sim 2\%$ of the typical values of the marginals $\langle m_{ua} \rangle$ for all values of C . The distribution of the normalized errors is in excellent agreement with a normal distribution with average 0 and standard deviation 1 (green line in bottom plots), indicating that most of the differences can be attributed to the sampling error.

the interval $]0, 1[$. In the stochastic case, the lower and upper bounds on the total capacity defined in (26) must be modified as

$$\hat{C}^- = \sum_u p_u \min_{a \in \partial u} w_{ua}, \quad \hat{C}^+ = \sum_u p_u \max_{a \in \partial u} w_{ua}. \quad (38)$$

Apart from this (minor) modification, the instance parameters affect the phenomenology of the problem in the same way as in the deterministic case discussed in Section V A.

B. Validation of the mirror approximation

We validated the mirror approximation described in Section VI A by comparing the average (over the realization of the t 's) of the marginals of the variables y_{ua} computed with the mirror approach with the same average marginals computed by sampling explicitly over the realization of the t 's. Specifically, we extracted one instance for each value of the parameters we tested, and we converged BP with the mirror fields to compute, for each edge $(ua) \in \mathbb{E}$, the marginal probability $m_{ua} = \mathbb{P}[y_{ua} = 2]$ that user u is served by service unit a , which is the relevant marginal for the computation of the observables we are interested in. We then extracted, for the same instances, 1000 realizations of the t 's, and for each realization computed the same marginal $m_{ua}^{(t)} = \mathbb{P}[y_{ua} = 2|t]$ with an ordinary BP (i.e. without mirror fields), and averaged them over the realizations of the t 's, obtaining the average value of the marginal \bar{m}_{ua} and its standard deviation σ_{ua} , representing the error on the estimate of \bar{p}_{ua} due to the finite size of the sampling.

In Figure 8 we show the distributions (over the edges $(ua) \in \mathbb{E}$) of both the absolute difference $\Delta_{ua} = m_{ua} - \bar{m}_{ua}$ between the mirror and sampling estimates of the marginals, and of their normalized error $\delta_{ua} = \Delta_{ua}/\sigma_{ua}$, for four instances with four different values of the capacity C (which is the most relevant parameter). In all cases, we find that the absolute difference is small compared to the typical value of the marginal $\langle m_{ua} \rangle = \sum_{(ua) \in \mathbb{E}} m_{ua}/|\mathbb{E}|$, and that the differences are mainly due to the sampling error.

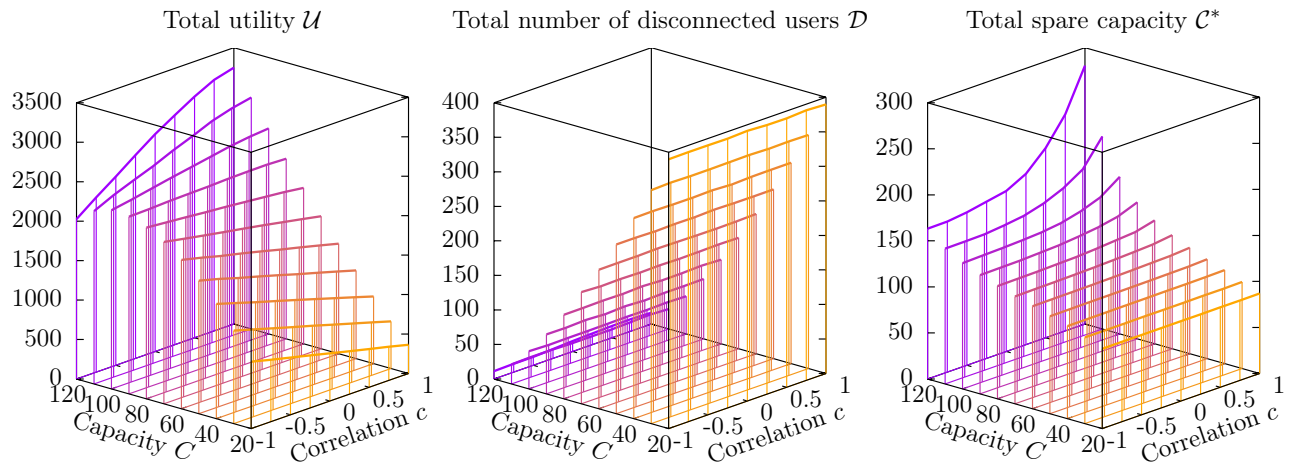


FIG. 9: Average values \mathcal{U} , \mathcal{D} and \mathcal{C}^* of the observables as a function of the capacity C_a of service units and the correlation c between weight and utility on individual edges. The other parameters are $N = 1000$, $M = 50$, $q = 0.1$, $w_{\min} = 6$, $w_{\max} = 15$, $v_{\min} = 1$ and $v_{\max} = 10$. Each data point, corresponding to a vertical line, is an average over 240 instances for $C \leq 100$, and over 40 to 120 instances for $C \geq 110$, and the standard deviations are of the order of the width of the lines. For $C = 120$ a significant number of instances did not converge, and were therefore excluded from the dataset.

C. Average values of U , D and C

As for the deterministic case, we study the average values of the relevant observables as a function of the capacity C of individual service units and of the correlation c between the weight w_{ua} and the utility u_{ua} on each edge $(ua) \in \mathbf{E}$. Once the range of capacities is rescaled to take into account both the smaller number of service units ($M = 50$ vs. $M = 200$ in the deterministic case) and the fact that the expected number of *active* users is $\bar{N} = 500$ (whereas all $N = 1000$ users are active in the deterministic case), we recover exactly the same phenomenology we observed in the deterministic case, and we refer the reader to Section V C for a discussion of the qualitative features of the numerical results shown in Figure 9.

D. Comparison with explicit dynamics

As for the deterministic case, we compare the average values of the observables obtained by averaging uniformly over all Nash equilibria with Belief Propagation with the results of the explicit simulation of three dynamics which converge to Nash equilibria:

- *Greedy (G)* – A list of active users is extracted based on the probabilities $\{p_u\}$ that each user u is active, and then we proceed as in the deterministic case for the active users
- *Best Response (BR)* – As for Greedy, we first extract a list of active users and then proceed as in the deterministic case for the active users
- *Arrivals/Departures (A/D)* – We consider a discrete time dynamics in which at each time step we extract a random permutation of all users, and then in the order of the permutation each active user becomes inactive with probability $(1 - p_u)/N$ while each inactive user becomes active with probability p_u/N and selects the best available service unit in a greedy way. At the end of each time step, Best Response is run until convergence for all active users in order to reach an equilibrium. The dynamics is repeated for a fixed number of time steps ($100 N$ in the numerical simulations).

Numerical results for the comparison are shown in Figure 10. As in the deterministic case, BP gives results that are very different from the three dynamics, which appear to be strongly biased towards “good” equilibria. Whereas in the deterministic case the BRB dynamics gives results that are significantly different from the other two (at least for some values of c), the A/D dynamics gives results which are quite similar to both G and BR, except for the number of disconnected users \mathcal{D} when $c \geq -0.5$. A detailed analysis on single instance following the steps of Section V D was not performed for the stochastic case.

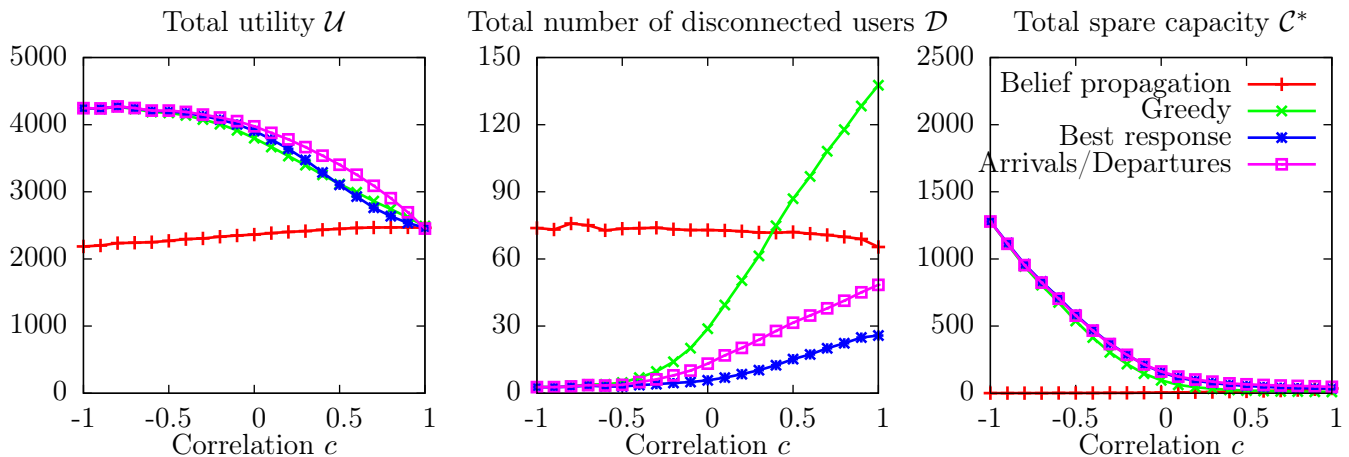


FIG. 10: Average values \mathcal{U} , \mathcal{D} and \mathcal{C}^* of the observables as a function of the correlation c between weight and utility on individual edges. The other parameters are $N = 1000$, $M = 50$, $C = 50$, $q = 0.1$, $w_{\min} = 6$, $w_{\max} = 15$, $v_{\min} = 1$ and $v_{\max} = 10$. Each data point is an average over ~ 70 instances, and for each instance, each dynamics is realized 30 000 times. The average value of each observable is computed over the instances and over the realizations. The standard deviations (of the averages over the realizations of the dynamics across different instances) are much smaller than symbol sizes, while the standard deviations (of the averages computed with Belief Propagation over the instances) is of the order of the symbol sizes.

VIII. CONCLUSIONS

We proposed a simple game theoretic model of distributed service provision, in which users want to be served by the service unit they prefer and they indirectly interact because of a capacity constraint. The existence of at least one Nash equilibrium is guaranteed by the fact that the game belongs to the class of potential games. The potential function is the total utility of the users and, for construction, the best response dynamics always converge to a local maximum of the potential, which is also a Nash equilibrium. The Nash equilibrium conditions can be rephrased as a set of hard constraints on configurations of binary variables (the choices of the users) and analyzed using standard statistical mechanics methods, such as belief propagation and message-passing algorithms. Moreover, a soft constraint in the form of an energetic term can be included in the factor graph formulation in order to study the properties of Nash equilibria with given average total utility. We derived belief propagation equations for this problem and studied the properties of the corresponding Nash equilibria on random instances of the service provision game, in which the user connectivity to the service units follows a Poisson distribution while the load weight provided by the users to the service units and the corresponding payoffs are drawn from a uniform distribution. The analysis of the Nash equilibrium landscape reveals a large variety of equilibria, with very different total utility. Best-response dynamics from random initial conditions usually tend to large-utility equilibria, even though those of smaller utility are exponentially more numerous. In order to prove that these equilibria can be actually reached by a simple dynamical process, we modified the best-response dynamics initializing it to a set of non-random initial configurations. These configurations are selected to be close to the saturation limit of the service unit capacities. In this regime, the rearrangement induced by the best response is very limited and the Nash equilibria obtained have a total utility close to the one of the initial configurations.

Other interesting phenomena appears when utility values and weights are correlated. The average total utility increases when the correlation c between weights and utility values increases, that is when the competition between users becomes harsher, whereas the opposite is observed in the low capacity regimes. Moreover, quite surprisingly the average spare capacity of Nash equilibria seems to increase with the correlation in the large capacity region. This means that, even if the users tend to choose the units on which they bring larger loads, they do it in a very optimized way. Our characterization of the equilibria also makes possible to estimate the price of anarchy of the game, which decreases smoothly from increasing the correlation.

In many realistic situations, the instance of the game theoretic problem changes over time, because the agents could follow very complex temporal activity patterns. In the absence of any precise information on the dynamics of the agents, the complexity of agents' activity is summarized into a set of stochastic parameters $\{t_u\}$, that indicate whether user u participate or not to the game. Users play a game on the deterministic instance corresponding to a single realization of the stochastic parameters, then the equilibrium properties should be averaged over different realizations of the parameters. Our results show that the average properties of the Nash equilibria in the stochastic case are qualitatively similar to those observed in the case of deterministic instances. However, our results are very

relevant from methodological viewpoint. In physical terms, the average over the stochastic parameters is a quenched average. Instead of resorting to sampling techniques, we put forward a systematic approximation scheme that, at least at the first-order level, can be naturally incorporated in the belief propagation approach by introducing some additional messages, that we call “mirror messages”. In the case under study, the method provides a very accurate estimate of all the average properties of interest. We believe that this approach could be useful to perform quench averages whenever the correlations between variables in the system are not too strong, however deeper investigations in this direction are necessary.

Acknowledgments

The authors acknowledge the European Grant ERC No. 267915 and Italian FIRB Project No. RBFR10QUW4.

-
- [1] N. Nisan, T. Roughgarden, E. Tardos, and V. V. Vazirani, *Algorithmic game theory* (Cambridge University Press, 2007).
 - [2] M. O. Jackson, *Social and economic networks* (Princeton University Press, 2010).
 - [3] E. Koutsoupias and C. Papadimitriou, in *STACS 99*, edited by C. Meinel and S. Tison (Springer Berlin Heidelberg, 1999), no. 1563 in Lecture Notes in Computer Science, p. 404413, ISBN 978-3-540-65691-3, 978-3-540-49116-3, URL http://link.springer.com/chapter/10.1007/3-540-49116-3_38.
 - [4] E. Anshelevich, A. Dasgupta, J. Kleinberg, . Tardos, T. Wexler, and T. Roughgarden, *SIAM Journal on Computing* **38**, 16021623 (2008), ISSN 0097-5397, URL <http://epubs.siam.org/doi/abs/10.1137/070680096>.
 - [5] L. Dall’Asta, P. Pin, and A. Ramezanzpour, *Journal of Public Economic Theory* **13**, 885901 (2011).
 - [6] L. Dall’Asta, P. Pin, and A. Ramezanzpour, *Physical Review E* **80**, 061136 (2009).
 - [7] A. Ramezanzpour, J. Realpe-Gomez, and R. Zecchina, *The European Physical Journal B-Condensed Matter and Complex Systems* **81**, 327339 (2011).
 - [8] M. Mézard and G. Parisi, *The European Physical Journal B - Condensed Matter and Complex Systems* **20**, 217233 (2001), ISSN 1434-6028, 1434-6036, URL <http://link.springer.com/article/10.1007/PL00011099>.
 - [9] M. Mézard and G. Parisi, *Journal of Statistical Physics* **111**, 134 (2003), ISSN 0022-4715, 1572-9613, URL <http://link.springer.com/article/10.1023/A%3A1022221005097>.
 - [10] M. Mézard and A. Montanari, *Information, Physics, and Computation* (Oxford University Press, 2009), ISBN 9780198570837.
 - [11] B. Vöcking, in *Algorithmic game theory* (Cambridge University Press, New York, 2007), p. 517542.
 - [12] R. W. Rosenthal, *International Journal of Game Theory* **2**, 6567 (1973), ISSN 0020-7276, 1432-1270, URL <http://link.springer.com/article/10.1007/BF01737559>.
 - [13] I. Milchtaich, *Games and economic behavior* **13**, 111124 (1996), URL <http://www.sciencedirect.com/science/article/pii/S0899825696900275>.
 - [14] D. Monderer and L. S. Shapley, *Games and economic behavior* **14**, 124143 (1996), URL <http://www.sciencedirect.com/science/article/pii/S0899825696900445>.
 - [15] T. Morita, *Journal of Mathematical Physics* **5**, 1401 (1964), URL <http://scitation.aip.org/content/aip/journal/jmp/5/10/10.1063/1.1704075>.
 - [16] R. Kühn, *Zeitschrift für Physik B Condensed Matter* **100**, 231242 (1996).
 - [17] J. S. Yedidia, W. T. Freeman, and Y. Weiss, in *NIPS 13* (MIT Press, 2000), p. 689695.
 - [18] J. S. Yedidia, W. T. Freeman, and Y. Weiss, in *Exploring Artificial Intelligence in the New Millennium*, edited by G. Lake-meyer and B. Nebel (Morgan Kaufmann Publishers Inc., San Francisco, CA, USA, 2003), p. 239269, ISBN 1-55860-811-7, URL <http://dl.acm.org/citation.cfm?id=779343.779352>.

